BERICHTE
DER
ARBEITSGRUPPE TECHNOMATHEMATIK

FORSCHUNG - AUSBILDUNG - WEITERBILDUNG

AN OVERVIEW OF THE METHOD OF SMOOTHED PARTICLE HYDRODYNAMICS

Joseph Peter Morris

Bericht 95 - 152 November 1995

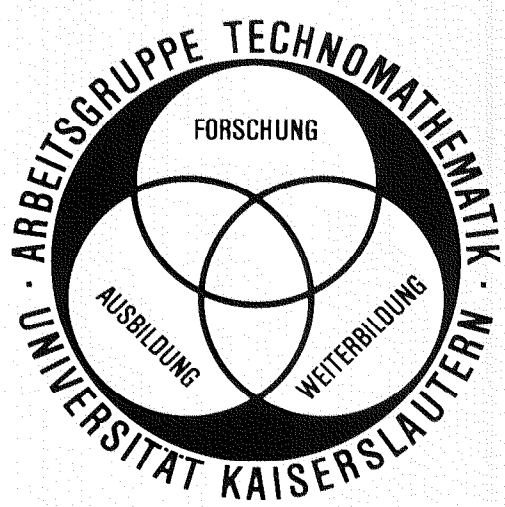

FACHBEREICH MATHEMATIK

An Overview of the Method of Smoothed Particle Hydrodynamics

Joseph Peter Morris
Universität Kaiserslautern
Fachbereich Mathematik
Postfach 3049
D -67653 Kaiserslautern

Permanent address:
Mathematics Department
Monash University
Clayton VIC 3168
email: jpm@fermat.maths.monash.edu.au

November 2, 1995

Abstract

This report is intended to provide an introduction to the method of Smoothed Particle Hydrodynamics or SPH. SPH is a very versatile, fully Lagrangian, particle based code for solving fluid dynamical problems. Many technical aspects of the method are explained which can then be employed to extend the application of SPH to new problems.

Contents

Chapter 1

Introduction

The numerical method, SPH, was first developed to model astrophysical problems ([8] and [5]). It has since been successfully applied to a vast range of problems, including elastic-plastic flow, MHD, incompressible flow and pyroclastic flow, to name a few. SPH is an extremely versatile method, however, the errors in results can sometimes be substantially larger than those obtained using methods specifically tailored for a given problem. There are many problems, though, which can only be practically handled by SPH. Problems where the geometry is highly irregular, or even dynamic, for example, are quite readily handled by SPH. It is hoped that this report will give the reader some insight into the potential of SPH and its limitations.

This report was written during the author's visit to the Department of Mathematics of the University of Kaiserslautern, Germany at the invitation of Professor Neunzert. The author gratefully acknowledges the support of the university, which made this report possible.

Chapter 2

The Fundamentals of SPH

This chapter is intended to introduce the reader to the concepts of SPH which are fundamental to the method. Similar introductions may be found in [11] and [3]. Slightly different approaches are used by each author to obtain essentially the same equations.

2.1 The basic idea

We start with the equation,

$$A(\mathbf{r}) = \int A(\mathbf{r}')\delta(\mathbf{r} - \mathbf{r}')d\mathbf{r}'. \tag{2.1}$$

If we replace the delta function by an interpolating kernel $W(\mathbf{r}, h)$ we obtain an integral interpolant of the function $A(\mathbf{r})$,

$$A_i(\mathbf{r}) = \int A(\mathbf{r}')W(\mathbf{r} - \mathbf{r}', h)d\mathbf{r}'. \tag{2.2}$$

The kernel W has the following properties,

$$\int W(\mathbf{r} - \mathbf{r}', h)d\mathbf{r}' = 1 \tag{2.3}$$

and

$$\lim_{h \to 0} W(\mathbf{r} - \mathbf{r}', h) = \delta(\mathbf{r} - \mathbf{r}'). \tag{2.4}$$

The integral interpolant, A_i, can be thought of a smoothed version of the original function A. This is the origin of "Smoothed" in SPH. The next step, is to approximate the integral interpolant with a summation interpolant over a number of points (particles) $\mathbf{r}_b$ in space:

$$A_s(\mathbf{r}) = \sum_b A_b \frac{m_b}{\rho_b} W(\mathbf{r} - \mathbf{r}_b, h). \tag{2.5}$$

The field quantities at particle b are denoted by a subscript b. The mass associated with particle b is m_b and so we see that the quantity $\frac{m_b}{\rho_b}$ is the inverse of the number density (ie- the specific volume) and is, in some sense, a volume element.

The density, for example, can be obtained using,

$$\rho(\mathbf{r}) = \sum_b m_b W(\mathbf{r} - \mathbf{r}_b, h). \tag{2.6}$$

It is now possible to obtain an estimate of the gradient of the field (provided W is differentiable) simply by differentiating the summation interpolant:

$$\nabla A_s(\mathbf{r}) = \sum_b A_b \frac{m_b}{\rho_b} \nabla W(\mathbf{r} - \mathbf{r}_b, h). \tag{2.7}$$

In practice, however, it is more accurate to use,

$$\nabla A = \frac{1}{\rho}\left[\nabla(\rho A) - A\nabla\rho\right], \tag{2.8}$$

$$= \frac{1}{\rho_a} \sum_b m_b (A_b - A_a) \nabla W(\mathbf{r} - \mathbf{r}_b, h), \tag{2.9}$$

since here the gradient of A is more explicit and thus is less susceptible to particle disorder. Similarly, while the divergence of $\mathbf{v}$ could be obtained using,

$$\nabla \cdot \mathbf{v} = \sum_b \frac{m_b}{\rho_b} \mathbf{v}_b \cdot \nabla W(\mathbf{r} - \mathbf{r}_b, h), \tag{2.10}$$

it is more accurate to use,

$$\nabla \cdot \mathbf{v} = \frac{\nabla \cdot (\rho \mathbf{v}) - \mathbf{v} \cdot \nabla \rho}{\rho} \tag{2.11}$$

$$= \frac{1}{\rho_a} \sum_b m_b (\mathbf{v}_b - \mathbf{v}_a) \cdot \nabla_a W(\mathbf{r} - \mathbf{r}_b, h). \tag{2.12}$$

For brevity, we will now introduce the notation,

$$W_{ab} = W(\mathbf{r}_a - \mathbf{r}_b, h), \tag{2.13}$$

and let $\nabla_a W_{ab}$ denote the gradient of W_{ab} taken with respect to $\mathbf{r}_a$ (the co-ordinates of particle a). Also, quantities such as $\mathbf{v}_a - \mathbf{v}_b$ shall be written $\mathbf{v}_{ab}$.

2.2 Modelling the Euler Equations

2.2.1 The Momentum Equation

If we move the particles with the velocity of the fluid, then,

$$\frac{d\mathbf{r}_a}{dt} = \mathbf{v}_a, \tag{2.14}$$

and

$$\frac{d\mathbf{v}_a}{dt} = -\frac{1}{\rho_a}(\nabla p)_a. \tag{2.15}$$

It is now a matter of choosing an SPH representation of the pressure gradient. We could use Eq. 2.9 and obtain,

$$(\nabla p)_a = \frac{1}{\rho_a}\sum_b m_b(p_b - p_a)\nabla_a W_{ab}. \tag{2.16}$$

For this expression, the force between particles is zero for constant pressure, and the stability properties (see Chapter 6) are quite appealing, but linear and angular momentum are not conserved exactly. If, however, we use,

$$\frac{\nabla p}{\rho} = \nabla(\frac{p}{\rho}) + \frac{p}{\rho^2}\nabla\rho, \tag{2.17}$$

then we have,

$$\frac{d\mathbf{v}_a}{dt} = -\sum_b m_b(\frac{p_a}{{\rho_a}^2} + \frac{p_b}{{\rho_b}^2})\nabla_a W_{ab}, \tag{2.18}$$

and linear and angular momentum are conserved exactly, since the particle forces are equal and opposite and act along the line joining their centres (provided that the kernel is symmetric). This form is also preferable because it is quite straightforward to obtain a consistent energy equation(see section 2.2.3), but there are many possible symmetric forms. The expression,

$$\frac{\nabla p}{\rho} = \frac{p}{\rho^\sigma}\nabla(\frac{1}{\rho^{1-\sigma}}) + \frac{1}{\rho^{2-\sigma}}\nabla(\frac{p}{\rho^{\sigma-1}}), \tag{2.19}$$

leads to,

$$\frac{d\mathbf{v}_a}{dt} = -\sum_b m_b\left(\frac{p_a}{{\rho_a}^\sigma {\rho_b}^{2-\sigma}} + \frac{p_b}{{\rho_b}^\sigma {\rho_a}^{2-\sigma}}\right)\nabla_a W_{ab}, \tag{2.20}$$

while,

$$\nabla p = 2\sqrt{p}\nabla\sqrt{p}, \tag{2.21}$$

gives,

$$\frac{d\mathbf{v}_a}{dt} = -\sum_b m_b\frac{2\sqrt{p_a}\sqrt{p_b}}{\rho_a\rho_b}\nabla_a W_{ab}. \tag{2.22}$$

2.2.2 The Continuity Equation

We can solve the continuity equation,

$$\frac{d\rho}{dt} = -\rho\nabla\cdot\mathbf{v}, \tag{2.23}$$

implicitly, taking advantage of the lagrangian motion of the particles using,

$$\rho_a = \sum_b m_b W_{ab}. \tag{2.24}$$

Since the number and masses of the particles remains constant, total mass is conserved. Under some circumstances, such as nearly incompressible flow (see Chapt. 4), it is better to use,

$$\frac{d\rho_a}{dt} = \sum_b m_b \mathbf{v}_{ab} \cdot \nabla_a W_{ab}, \tag{2.25}$$

since this allows the densities to be set at each particle and may be employed to eliminate oscillations at free surfaces. Also, normally the density must be obtained first by a sum over all the particles before other quantities may be interpolated (involving a second pass over the particles). Having a differential equation for ρ means that it can be updated at the same time as other particle quantities and only one pass over the particles is required to obtain all the required information. The main disadvantage is that this expression does not conserve mass exactly, but this does not cause problems in many applications. It can be computationally advantageous to use Eq. 2.25 for several time steps and then correct the density by using Eq. 2.24

Sources and sinks of matter are quite readily introduced. Consider a continuity equation of the form,

$$\frac{d\rho}{dt} = -\rho \nabla \cdot \mathbf{v} + f(\mathbf{r}). \tag{2.26}$$

Since, total mass is no longer conserved, the particle masses must be allowed to vary with time. Taking the time derivative of Eq. 2.24 we find,

$$\frac{d\rho_a}{dt} = \sum_b m_b \frac{dW_{ab}}{dt} + \sum_b \frac{dm_b}{dt} W_{ab}. \tag{2.27}$$

Since the SPH expression for Eq. 2.26 is,

$$\frac{d\rho_a}{dt} = \sum_b m_b \mathbf{v}_{ab} \cdot \nabla_a W_{ab} + \sum_b \frac{m_b}{\rho_b} f_b W_{ab}, \tag{2.28}$$

we formally make the identification,

$$\frac{dm_b}{dt} = \frac{m_b}{\rho_b} f_b. \tag{2.29}$$

2.2.3 The Thermal Energy Equation

We start with the equation for the evolution of thermal energy per unit mass,

$$\frac{du}{dt} = -(\frac{p}{\rho}) \nabla \cdot \mathbf{v}. \tag{2.30}$$

We can simply translate this (using Eq. 2.12) to the SPH expression,

$$\frac{du_a}{dt} = (\frac{p_a}{{\rho_a}^2}) \sum_b \mathbf{v}_{ab} \cdot \nabla_a W_{ab}, \tag{2.31}$$

when using Eq. 2.18, this conserves total energy exactly. To see this, we must consider the rate of change of kinetic energy resulting from Eq. 2.18. The total kinetic energy of the particles is,

$$E_k = \sum_a \frac{1}{2} m_a {\mathbf{v}_a}^2, \tag{2.32}$$

so the time rate of change is given by,

$$\begin{aligned}
\frac{dE_k}{dt} &= \sum_a m_a \mathbf{v}_a \cdot \frac{d\mathbf{v}_a}{dt}, & (2.33)\\
&= \sum_a m_a \mathbf{v}_a \cdot \{-\sum_b m_b (\frac{p_a}{{\rho_a}^2} + \frac{p_b}{{\rho_b}^2}) \nabla_a W_{ab}\}, & (2.34)\\
&= -\sum_a \sum_b m_a m_b (\frac{p_a}{{\rho_a}^2} + \frac{p_b}{{\rho_b}^2}) \mathbf{v}_a \cdot \nabla_a W_{ab}. & (2.35)
\end{aligned}$$

Simply swapping the dummy indices we obtain,

$$\begin{aligned}
\frac{dE_k}{dt} &= -\sum_b \sum_a m_b m_a (\frac{p_b}{{\rho_b}^2} + \frac{p_a}{{\rho_a}^2}) \mathbf{v}_b \cdot \nabla_b W_{ba}, & (2.36)\\
&= -\sum_b \sum_a m_b m_a (\frac{p_b}{{\rho_b}^2} + \frac{p_a}{{\rho_a}^2}) \mathbf{v}_b \cdot (-\nabla_a W_{ab}), & (2.37)
\end{aligned}$$

since $\nabla_b W_{ba} = -\nabla_a W_{ab}$ by antisymmetry. Thus, we can combine these results to get a symmetric form and write,

$$\frac{dE_k}{dt} = -\frac{1}{2} \sum_a m_a \sum_b m_b (\frac{p_a}{{\rho_a}^2} + \frac{p_b}{{\rho_b}^2}) \mathbf{v}_{ab} \cdot \nabla_a W_{ab}. \tag{2.38}$$

Similarly, the time rate of change of the total internal energy resulting from Eq. 2.31 is,

$$\begin{aligned}
\frac{dU}{dt} &= \frac{d}{dt} \sum_a m_a u_a, & (2.39)\\
&= \sum_a \sum_b m_a m_b \frac{p_a}{{\rho_a}^2} \mathbf{v}_{ab} \cdot \nabla_a W_{ab}, & (2.40)\\
&= \sum_a \sum_b m_a m_b \frac{p_b}{{\rho_b}^2} \mathbf{v}_{ba} \cdot \nabla_b W_{ba}, & (2.41)\\
&= \frac{1}{2} \sum_a m_a \sum_b m_b (\frac{p_a}{{\rho_a}^2} + \frac{p_b}{{\rho_b}^2}) \mathbf{v}_{ab} \cdot \nabla_a W_{ab}. & (2.42)
\end{aligned}$$

Total energy is conserved since it is the sum of the kinetic and internal energy of the particles.

There are other possible choices for updating the internal energy of the particles. For example (see [11]),

$$\frac{du_a}{dt} = \sum_b m_b \frac{1}{2}\left(\frac{p_a}{{\rho_a}^2} + \frac{p_b}{{\rho_b}^2}\right)\mathbf{v}_{ab} \cdot \nabla_a W_{ab}, \tag{2.43}$$

is preferred by some because it has similar symmetric factors to Eq. 2.18. In [3], however, it is pointed out that this form, while conserving total energy, can, in some circumstances, overestimate the rate of change of internal energy.

2.3 The Artificial Viscosity

If we model the Euler equations with any method at finite resolution without some sort of viscosity, low order diffusion or a Riemann solver, we find large, unphysical oscillations are generated downstream of shocks. In the case of SPH, it is easiest to introduce an artificial viscosity, though some work has been done involving Riemann solvers (e.g. GPH, or Goudonov SPH). Many forms of artificial viscosity have been proposed, but the most commonly used is the following, viscous "pressure",

$$\Pi_{ab} = \begin{cases} \frac{-\alpha \bar{c} \mu_{ab} + \beta {\mu_{ab}}^2}{\bar{\rho}}_{ab}, & \text{if } \mathbf{v}_{ab} \cdot \mathbf{r}_{ab} < 0; \\ 0, & \text{otherwise,} \end{cases} \tag{2.44}$$

where,

$$\mu_{ab} = \frac{h \mathbf{v}_{ab} \cdot \mathbf{r}_{ab}}{{\mathbf{r}_{ab}}^2 + 0.01h^2}, \tag{2.45}$$

and $\bar{\rho}_{ab} = \frac{1}{2}(\rho_a + \rho_b)$ and $\bar{c}_{ab} = \frac{1}{2}(c_a + c_b)$. Here c_a denotes the sound speed at particle a. The $0.01h^2$ in the denominator is included to keep the viscosity bounded for particles as they approach. This viscous "pressure" is incorporated into the SPH momentum equation,

$$\frac{d\mathbf{v}_a}{dt} = -\sum_b m_b \left(\frac{p_a}{{\rho_a}^2} + \frac{p_b}{{\rho_b}^2} + \Pi_{ab}\right)\nabla_a W_{ab}, \tag{2.46}$$

and (by conservation of energy) introduces a new source term in the internal energy equation,

$$\frac{du_a}{dt} = \left(\frac{p_a}{{\rho_a}^2}\right)\sum_b \mathbf{v}_{ab} \cdot \nabla_a W_{ab}, + \frac{1}{2}\sum_b m_b \Pi_{ab} \mathbf{v}_{ab} \cdot \nabla_a W_{ab}. \tag{2.47}$$

The viscosity, in this form, is intended only to provide the dissipation needed at a shock to convert kinetic energy into internal energy. Hence, the viscosity is

only active for approaching particles. It can be shown (see [9]) that the viscosity associated with the α coefficient produces a shear and bulk viscosity. The β term (quadratic in μ_{ab}) is necessary to provide sufficient damping in high Mach number shocks.

The viscosity can, however, cause problems in regions of high shear. Here particles are in relative motion, but one does not wish this motion to be critically damped. There are different approaches to correcting this problem, but most involve using some sort of switch which detects the presence of a shock. One possibility is to use a modified μ_{ab}, say μ^*_{ab}, defined,

$$\mu^*_{ab} = \mu_{ab}\frac{f_a + f_b}{2}, \tag{2.48}$$

where,

$$f_a = \frac{|(\nabla \cdot \mathbf{v})_a|}{|(\nabla \cdot \mathbf{v})_a| + |(\nabla \times \mathbf{v})_a| + 0.0001\frac{c_a}{h}}. \tag{2.49}$$

The idea here is to "concoct" a term which goes to zero for pure shear flows (where divergence is zero, but curl is not). This may seem ad hoc, and in some sense it is, but the artificial viscosity itself is a necessary evil which was not present in the Euler equations. It is also possible to evolve α and β in time, so that viscosity is introduced only at significant shock fronts([18]), but this is still under development.

2.4 Thermal Conduction

Heat conduction may be introduced to a simulation either because it is present in the physics of the real problem, or because it is needed to reduce excess heating (for example when cold streams of gas collide). The standard differential equation for head conduction is,

$$\frac{\partial u}{\partial t} = \frac{1}{\rho}\nabla \cdot \kappa \nabla u, \tag{2.50}$$

where κ is the thermal conductivity. One could attempt to convert this directly into an SPH form, but it would either require two sweeps over the particles (one for each gradient) or directly involve second order derivatives. Estimation of second order derivatives with SPH approximations which use second order derivatives of the kernel are very sensitive to particle disorder. So an alternative expression has been developed, which only employs the gradient of the kernel,

$$\frac{\partial u_a}{\partial t} = \sum_b \frac{m_b(\kappa_a + \kappa_b)(u_a - u_b)\mathbf{r}_{ab} \cdot \nabla_a W_{ab}}{\rho_a \rho_b ({\mathbf{r}_{ab}}^2 + 0.01h^2)}. \tag{2.51}$$

It can be shown, ([13]) by taking a Taylor expansion about a particle, that this does reduce to the heat equation. The contributions particles make to each other's heat fluxes are antisymmetric, so total heat is conserved.

If the conduction is intended to be artificial, it may be more convenient to use

$$\frac{\partial u_a}{\partial t} = \sum_b \frac{m_b(q_a + q_b)(u_a - u_b)\mathbf{r}_{ab} \cdot \nabla_a W_{ab}}{\bar{\rho}_{ab}(\mathbf{r}_{ab}{}^2 + 0.01h^2)}, \tag{2.52}$$

where $q = \kappa/\rho$ has the dimension of length squared per unit time. This allows us to readily introduce conduction where it is needed by replacing $q_a + q_b$ with $\frac{1}{2}h(\bar{c}_{ab} + 4|\mu_{ab}|)$. This term is intended to provide conduction in those regions of the flow where large amounts of compression (shocking) occurs, but could be improved upon by taking a similar approach to that outlined in Section 2.3 for shock detection.

2.5 The Choice of Kernel

Theoretically, the choice of kernel is arbitrary, provided it satisfies equations 2.3 and 2.4. We will consider kernels of the form,

$$W(r,h) = \frac{1}{h^\nu} f(\frac{r}{h}), \tag{2.53}$$

where ν is the number of dimensions. The requirements of Eq. 2.3 and Eq. 2.4 can then be written,

$$\int f(s)dV = 1, \tag{2.54}$$

and,

$$\lim_{h \to 0} f(\frac{r}{h}) = \delta(r), \tag{2.55}$$

respectively. Here dV, the volume element, is ds, $2\pi s ds$ or $4\pi s^2 ds$ in one, two or three dimensions respectively.

In practice, there are many, sometimes competing, factors to be considered when choosing a kernel for your SPH code. The main considerations are the order of interpolation, the number of nearest neighbours, and the symmetry and stability properties. Using a tent function as the kernel, for example, is not a good idea, since, while having compact support, and being symmetric, the resulting technique is unstable to most positive stresses and induces a non-physical sound speed for negative stresses (see Eq. 6.4).

The original work using SPH employed a Gaussian kernel (here normalised for one dimension),

$$f_{\mathcal{G}}(s) = \frac{1}{\sqrt{\pi}} \exp(-s^2). \tag{2.56}$$

This kernel has many attractive properties. The Gaussian in higher dimensions is the product of lower dimensional Gaussians. Its derivative involves itself,

$$\frac{df_{\mathcal{G}}}{ds} = -2s f_{\mathcal{G}}, \tag{2.57}$$

making some analysis much simpler, and its Fourier transform is, itself, a Gaussian. This last point is most important with respect to stability properties of the resulting numerical method(see [19] and Chapter 6). The Gaussian, however, does not have compact support, so all particles make (mostly vanishingly small) contributions to each other in the summations.

Most simulations today use the cubic spline interpolated kernel (here normalised for one dimension),

$$f(s) = \frac{1}{h} \begin{cases} \frac{2}{3} - s^2 + \frac{1}{2}s^3, & \text{if } 0 \leq s \leq 1; \\ \frac{1}{6}(2-s)^3, & \text{if } 1 \leq s \leq 2; \\ 0, & \text{if } s \geq 2. \end{cases} \tag{2.58}$$

The cubic spline interpolated kernel was introduced (see [17]), since (having compact support) a potentially small number of neighbouring particles are the only contributors in the sums over the particles. This is, of course, a great computational advantage. However, it has been shown(see [19] and Chapter 6) that the dispersion relation for linear waves in a lattice of SPH particles has some undesirable properties if the cubic spline interpolant is used. These problems can be negligible, however, depending on the application. The quartic spline,

$$f(s) = A_4 \begin{cases} (s+2.5)^4 - 5(s+1.5)^4 + 10(s+0.5)^4, & \text{if } 0 \leq s < 0.5; \\ (2.5-s)^4 - 5(1.5-s)^4, & \text{if } 0.5 \leq s < 1.5; \\ (2.5-s)^4 & \text{if, } 1.5 \leq s < 2.5; \\ 0, & \text{if } s \geq 2.5, \end{cases} \tag{2.59}$$

and quintic spline

$$f(s) = A_5 \begin{cases} (3-s)^5 - 6(2-s)^5 + 15(1-s)^5, & \text{if } 0 \leq s < 1; \\ (3-s)^5 - 6(2-s)^5, & \text{if } 1 \leq s < 2; \\ (3-s)^5, & \text{if } 2 \leq s < 3; \\ 0, & \text{if } s \geq 3, \end{cases} \tag{2.60}$$

interpolants, have progressively better stability properties, but at an increased computational cost, since the region of contributing neighbours is larger. Here A_4 and A_5 are normalisation constants.

Simply on account of their symmetry, all of these kernels interpolate to order h^2 accuracy (since all odd moments are eliminated). It is possible, to formulate kernels which interpolate to higher order accuracy by cancelling higher order moments in s. One such kernel is the super-Gaussian (see [6]). To my knowledge, not much work has been done regarding the advantages and disadvantages of such kernels. One possible disadvantage is that the kernel is negative in a region of its domain and, thus, ρ_a obtained by Eq. 2.24 could be negative in some circumstances.

2.6 Variable Smoothing Length

Changing the smoothing length in SPH corresponds to changing the numerical resolution. If the fluid modelled does not undergo substantial compression or rarefaction, constant h is sufficient. If particles become so distant, that they cease to interact, or so close that a large number are within a smoothing length, h should be changed accordingly. All of the interpolation used by SPH depends on having a sufficient number of particles within a smoothing length and the speed of the computation depends on this number being relatively small. In one dimension the number of neighbours (including the "home" particle itself) should be about 5. In two dimensions, it should be about 21 and in three dimensions, about 57. These numbers all correspond to the number of neighbours on a cubic lattice with a smoothing length of 1.2 times the particle spacing, and a kernel which extends to $2h$ (such as the cubic spline). There are many ways to dynamically change h such that the number of neighbours is kept relatively constant.

The simplest approach is to let,

$$h_a = h_0(\frac{\rho_0}{\rho_a})^{\frac{1}{\nu}}, \tag{2.61}$$

where ν is the number of dimensions. This only really makes sense if the particles are of equal masses, since ρ is being used here as an estimate of the number density. The trouble with this approach is that it requires ρ_a to be known, before h_a can be known, but h_a must be used to obtain ρ_a! The ρ_a could be used from the previous step, but this results in the smoothing length responding too slowly as a particle enters a shock. An interesting, and successful approach, suggested by [3] is to take the time derivative of Eq. 2.61 and substitute the continuity equation,

$$\frac{dh}{dt} = -\frac{1}{\nu}\frac{h}{\rho}\frac{d\rho}{dt} \tag{2.62}$$

$$= \frac{1}{\nu}h\nabla\cdot\mathbf{v} \tag{2.63}$$

This equation can then be integrated along side the other differential equations. It may be prudent to reset h_a according to Eq. 2.61 occasionally, so ensure the time integration of h_a is not "wandering".

Since each particle now has its own smoothing length, each particle pair interaction, must have a smoothing length h_{ab} associated with it. If we wish to conserve momentum exactly, this must be done in such a way as to preserve the former symmetry of particle interactions:

$$W_{ab} = W(r_{ab}, h_{ab}), \tag{2.64}$$

where,

$$h_{ab} = \frac{1}{2}(h_a + h_b), \tag{2.65}$$

$$h_{ab} = min(h_a, h_b), \tag{2.66}$$
$$h_{ab} = max(h_a, h_b), \tag{2.67}$$
$$\text{or } h_{ab} = \frac{h_a h_b}{(h_a + h_b)}, \tag{2.68}$$

or we can average the kernels,

$$W = \frac{1}{2}(W(h_a) + W(h_b)). \tag{2.69}$$

There are advantages and disadvantages to using each of these. For example, for the arithmetic mean in the limit of h_a being dominant, $h_{ab} \approx \frac{1}{2}h_a$. This means that if, somehow, a particle has an anomalously large h, it can overly smooth out interactions with surrounding particles. This applies too, for taking the maximum of the smoothing lengths. The geometric mean, however, tends to h_b as h_a becomes large, so the resolution of the method is kept small. This also applies for taking the minimum. It is possible, however, that this approach may deprive a particle of the required number of neighbours. Taking an average of the kernels may be a good compromise, but I am not aware of a detailed comparison of these approaches. In anycase, if variable smoothing length is being employed, the results obtained should be invariant to the method used, provided the method has converged. The choice of combined smoothing length also effects the speed with which nearest neighbours can be located (see Section 3.2).

It should also be pointed out that it is not entirely consistent to allow h to vary in space and time. The original SPH equations of motion were derived assuming h was a constant. It is possible to rederive the SPH approximations, allowing h to vary (see [4] and [11]). It has been found that, provided h varies on a scale similar to other variables, the errors are of $O(h^2)$ (see [7]).

2.7 Initialising the Particles

As with any particle method, initialising SPH particles can sometimes take quite a bit of effort. In some cases, however, this may be because the initial conditions themselves are somewhat "artificial". In most situations, we attempt to construct a "quiet" start. That is, a configuration of particles which does not have too much internal energy due to particles being placed in "unnatural" ways. The approach taken depends very much on the precise application, but there are some basic considerations to keep in mind.

If the initial conditions involve discontinuities (either a shock or a contact discontinuity), the interpolation used by SPH will smooth them out. This, typically, will lead to some extra particle motion at the interface as the SPH particles respond to the pressure gradients induced by the smoothed fields. If Eq. 2.18 is used, we see that, even if the pressure is constant everywhere, for the total

force on each particle to be zero, all other particles must be placed symmetrically about eachother. In particular, at a contact discontinuity, where either the particle spacing or particle masses will change, it is almost impossible to have an absolutely quiet start. The noise can be minimised, however, by smoothing the initial conditions. In the case of incompressible SPH (see Chapter. 4) these problems are avoided by using Eq. 2.25, setting the density everywhere and subtracting the background pressure.

It may be convenient to place particles on a regular lattice, but care must be taken. Such a lattice will have directions along which particles form straight lines. Compression along these such axes will cause particles to squeeze up into a dense line. If h is being changed in response to this compression, particles may lose "sight" of neighbours in parallel lines of particles. In anycase, the forces along such lines are artificially large, and eventually such lines buckle, releasing substantial energy. If the initial velocity field naturally disturbs the initial, regular lattice, these problems may be negligible.

Placing particles in a purely random fashion is certainly not advisable, since this results in a great deal of noise which viscosity will convert into internal energy. As a compromise, however, it is possible to use generalised Halton sequences (or some other infinite sequences) to choose the particle positions. Most such sequences select points in a unit interval. In many problems it is quite straight forward to develop a transformation which will transform a constant density on a unit interval to the desired density field. Residual noise may be removed by introducing a relaxation term to the equations of motion, until the configuration has settled:

$$\frac{d\mathbf{v}}{dt} = -\Gamma\mathbf{v} + \mathbf{F}. \tag{2.70}$$

Here Γ is the co-efficient of the damping and $\mathbf{F}$ includes the standard forces.

Chapter 3

The Nearest Neighbour Problem

It has already been mentioned that, in practice, kernels with compact support are used in SPH simulations. This is so that each particle has a *finite* number of "neighbouring" particles which make non-zero contributions to it. The problem still remains, however, to quickly find these interacting particles. There are several solutions to this problem, and the optimal algorithm will depend on the nature of the problem being solved. Here, we will consider methods which assume that the SPH interactions are the only ones which need to be calculated. If, for example, SPH is being used to provide hydrodynamics within a self-gravitating problem being solved by a hierarchical tree-code, the same structures used by the tree-code to organise the gravitational approximations can readily be used to find nearest neighbours to SPH particles. The methods we will consider involve creating a collection of cells which cover real space and allow us to order and locate particles in space. These cells, or grid, are simply used as a means of locating particles, and do not effect the results of the simulation, only the speed with which it is obtained. Let us first consider the simpler case of constant smoothing length.

3.1 Locating neighbours with h constant

In this case, all particles have the same "interaction radius",

$$r_0 = s_k h_0, \tag{3.1}$$

where s_k is the "extent" of the kernel in the co-ordinate $s = r/h_0$. We can then divide the computational domain into cells of width r_0, and create lists of particles belonging to each cell. A particle within a given cell, then, need only consider interactions with particles in neighbouring cells. The lists of particles within each cell are most easily implemented as linked lists. That is, there is a pointer to the first particle in a cell, and that particle then points to the second particle and so on.

Let us consider the algorithm for one dimension in detail.

for $i = 1$ to n do
    $j = int((x_i - x_{min})/r_0)$
    $next_i = head_j$
    $head_j = i$

Here $head_j$ is a pointer to the first particle in cell j, and is initially set to 0, while $next_i$ is a pointer from particle i to the next particle in the linked list. Note that $head_j$ will point to 0 if cell j is empty and $next_i$ will point to 0 if it is the last particle in the list. Finding nearest neighbours of particles i in cell j is now a much cheaper operation:

for $cell = j - 1$ to $j + 1$ do
    $k = head_{cell}$
    while $(k \neq 0)$ do
        consider particle k
        $k = next_k$

However, in practice we do not consider an individual particle and search for its nearest neighbours. It is much more efficient to create a temporary list of particles in a given cell and interacting neighbouring cells and evaluate the interactions between them. Also, since we need only consider each pair of particles once, it is enough to consider the neighbouring cell to one side of our home cell. We do this safe in the knowledge that the cell on the other side will consider our home cell as its neighbour and include it. For example, considering the SPH interactions for cell j, we create a list of particles from cell j (the home cell) and cell $j + 1$ (the neighbouring cell to the right):

    $i = 0$
    $k = head_j$
    while $(k \neq 0)$ do
        $i = i + 1$
        $list_i = k$
        $k = next_k$
    $n_{home} = i$
    $k = head_{j+1}$
    while $(k \neq 0)$ do
        $i = i + 1$
        $list_i = k$
        $k = next_k$
    $n_{total} = i$

The SPH contributions can be readily obtained by considering the pairs:

for $i_1 = 1$ to n_{home} do
  $a = list_{i_1}$
  for $i_2 = i_1$ to n_{total} do
    $b = list_{i_2}$
    consider particle a and b

This loop considers all the interactions between particles in the home cell (j) with eachother and with those particles in the neighbouring cell ($j+1$). Since we don't wish to consider the interactions between particles in the neighbouring cell with themselves, the first loop is over n_{home} particles while the second is over n_{total} particles.

3.2 Locating neighbours with variable h

Once h is allowed to vary, the interaction radius for each particle is different. In fact since we must apply some rule to obtain the effective h for a pair of particles, the interaction radius will be different for each pair of particles in general. Some of the ways smoothing lengths can be combined have been mentioned previously:

$$h_{ab} = \frac{1}{2}(h_a + h_b), \tag{3.2}$$

$$h_{ab} = min(h_a, h_b), \tag{3.3}$$

$$h_{ab} = max(h_a, h_b), \tag{3.4}$$

$$h_{ab} = \frac{h_a h_b}{(h_a + h_b)}, \tag{3.5}$$

or we can average the kernels,

$$W = \frac{1}{2}(W(h_a) + W(h_b)). \tag{3.6}$$

I have only listed symmetric combinations, as I'm assuming that exact conservation of momentum is desired. In any case, the interaction length, for a pair of particles is:

$$r_{ab} = s_k h_{ab}. \tag{3.7}$$

Now, if h does not vary by much in the simulation, it may be feasible to use the approach described in the previous section, taking:

$$r_0 = max(r_{ab}). \tag{3.8}$$

However, as the variation in h is increased, there will be regions where large numbers of particles (with small h) are clustered into single cells. Calculating

the interactions between these particles is very expensive. Essentially, we much stretch the cell sizes according to the number density of the particles. When using constant h, the cell boundaries are equispaced in real space, since the particles are equispaced in real space. The most straight forward way to extend this (using a Cartesian grid) is to consider cell boundaries which are equispaced in particle rank space. That is, if we consider the particles ranked from left-most (say) to right-most (ie- rank listed in x), the cell boundaries occur between every n_{cell}-th particle. The choice of n_{cell} is made such that it is expected that one or two particles will be in each cell. In two dimensions, for example, $n_{cell} = \sqrt{n}$ may be a good choice.

So, firstly, the particles must be sorted lowest to highest in each dimension. The particles must also be sorted at each time step, to obtain the new rank list and thence the cell grid. There are many algorithms for sorting lists and they each have their advantages and disadvantages. Quicksort, for example, can be very slow at sorting data which is nearly in order. Since we expect the particle rankings to remain very similar from one time-step to the next, quicksort is probably not a good choice. Some sort of insertion sort may be best, provided new particles are not being introduced or old particles deleted from the solution. Even regions of substantial overturning may cause an insertion sort to become too expensive. Heap sort, however, always takes $O(n\log(n))$ and thus provides reliable, fast rankings of the particles. Once the particles are sorted, the cell boundaries can be readily determined. As the cell boundaries are determined, particles can also be assigned to cells. It is useful at this point to record the maximum h (h_{max}) for each cell.

The algorithm now proceeds in a fashion analogous to that of that for constant h with some complications. To find the interacting neighbours about a given particle, we must consider all other cells which could contain interacting particles. At this point, our choice for obtaining h_{ab} is crucial. To make this clear it is simplest to consider the extremes. If we use $h_{ab} = max(h_a, h_b)$, then particle a does not "know" a priori if nearby, but outside $s_k h_a$ there is a particle b with sufficiently large h_b such that the two particles interact. If we use $h_{ab} = min(h_a, h_b)$, then particle a "knows" that no other particle interaction can increase the interaction radius beyond $s_k h_a$. Thus, in the latter case, a given particle "knows" the maximum volume of space it must search for its neighbours.

Using the maximum h approach, we do not know how far to search about a given particle for neighbours, unless we know that this particle is that with the largest h. So, we consider the particles in turn from largest h to smallest and only consider reciprocal contributions with particles of a smaller h.

If we are using the minimum h approach, then for a given home cell we can readily collect the particles from those neighbouring cells within $s_k h_{max}$ of the home cell. This then allows us to consider the SPH interactions in a cell-by-cell approach, which is faster than considering the interactions particle-by-particle. In the latter approach one is forced to access the data of each cell many more

times looking for neighbours.

It has already been pointed out, however, that the minimum h approach may be less accurate under certain circumstances. Yet, the speed of the algorithm, may allow the resolution to be increased and these relative inaccuracies eliminated.

Under many circumstances, a Cartesian structure for the cells may not be optimal. For example, if matter is concentrated in a spherical fashion, ranking the particles in a spherical co-ordinate system may be faster. Using either structure correctly, the results should be identical though. It's a matter of how much time is spent obtaining them.

Chapter 4

Free Surface Flows

4.1 Some Background

The approach usually taken when modelling fluids with very high sound speeds, such as water, is to assume the fluid is actually incompressible. With SPH, since is was designed for compressible flows, it is easier to model such flows using a fluid which is slightly compressible. If we do a scale analysis of the momentum equation, we find,

$$\frac{\delta\rho}{\rho} \sim \frac{vL}{c^2\tau}, \tag{4.1}$$

where ρ, v, L, τ and c are typical density, velocity, length, time scale and sound speed respectively. The fractional variation in density is $\delta\rho/\rho$. Now, if $v \sim L/\tau$ then we have,

$$\frac{\delta\rho}{\rho} \sim (\frac{v}{c})^2 = M^2, \tag{4.2}$$

where $M = v/c$ is the Mach number. So, if we wish the relative density fluctuations to be about 1% then we must choose our sound speed to give a Mach number of 1/10. The near-incompressible formulation of SPH has been applied successfully to the modelling of bursting dams, bores, wave makers ([12]) and gravity currents ([15]).

4.2 Modifications of the SPH Equations

There are some minor modifications which should be made in order to model free surface flows. Firstly, if Eq. 2.24 is used to obtain the density, the discontinuity at the fluid surface is smoothed over a distance of $O(h)$, introducing large pressure gradients. These, in turn, cause the surface to oscillate violently. It is better, then, to use Eq. 2.25, since this allows us to set the density correctly initially. This equation will modify the density according to the relative motion of the particles.

Normally, we move the particles using Eq. 2.14, but for free-surface problems it can be better to use the XSPH variant (see [10]), where,

$$\frac{d\mathbf{r}_a}{dt} = \hat{\mathbf{v}}_a = \mathbf{v}_a + \epsilon \sum_b m_b (\frac{\mathbf{v}_{ba}}{\bar{\rho}_{ab}}) W_{ab}. \tag{4.3}$$

Here, $\hat{\mathbf{v}}_a$ is a smoothed velocity which includes contributions from the surrounding velocity field. It is found that this approach keeps the particles more orderly and, in high speed flows, prevents fluids interpenetrating. For consistency, $\hat{\mathbf{v}}_a$ should be used in place of $\mathbf{v}_a$ in Eq. 2.25. In relatively gentle flows, taking $\epsilon = 0$ is possible, but in more active flows, taking $\epsilon = 1/2$ can be necessary. All of the flows modelled in [12] use $\epsilon = 1/2$. There is some further discussion of the XSPH formulation in [3] and [11]. The XSPH approach can be useful in compressible problems also, where it is used to reduce particle penetration and improves modelling of shear layers.

The final modification we must consider is that of the equation of state. The one most commonly used for these applications is based on an equation of state for water given in [1],

$$p_a = p_0((\frac{\rho_a}{\rho_0})^7 - 1). \tag{4.4}$$

The "-1" is necessary, since particles at the interface do not have particles "outside" to exert a force back on them. The subtraction of p_0 thus models an external pressure. We choose p_0 such that the sound speed,

$$c = \sqrt{\frac{\partial p}{\partial \rho}} \approx \sqrt{\frac{7p_0}{\rho_0}} \tag{4.5}$$

is suitably large. Suppose that v_{typ} is a typical bulk velocity in the problem we are considering. Then, from the previous discussion (Eq. 4.2), we require that $c \approx 10 v_{typ}$. This gives,

$$p_0 \approx \frac{100 {v_{typ}}^2 \rho_0}{7}. \tag{4.6}$$

In the case of a bursting dam of height H, by conservation of energy, we expect,

$$v_{typ} = \sqrt{2gH}, \tag{4.7}$$

so, in this case,

$$p_0 \approx \frac{200 \rho_0 g H}{7}. \tag{4.8}$$

It should also be mentioned that it is not advisable to use a very small smoothing length. Since the equation of state is so hard, if particles are to move past eachother the smoothing length may need to be a little longer than is normally necessary. Taking $h \approx 1.5\Delta x$ (where Δx is the typical distance between particles) is certainly adequate (for the cubic spline kernel). A small amount of viscosity should also me used. Typically, $\alpha \approx 0.01$ is sufficient ($\beta = 0$). Since the viscosity scales with the sound speed (see Eq. 2.44), it is important that α be small.

4.3 The Initial Conditions

Particular care should be taken initialising problems involving a nearly incompressible fluid. Clearly, a small error in the initial setup can introduce significant amounts of energy when the equation of state is so hard. As has been mentioned previously, we set the density at each particle and allow Eq. 2.25 to determine the evolution of the densities. Since the equation of state (Eq. 4.4) has the background pressure subtracted, particles at the edge of the fluid, do not feel an unbalanced outwards force. Thus, we need only consider how the density must be chosen to balance body forces. For example, if we consider a body of water of depth H, to balance gravity we must have hydrostatic support,

$$\frac{dp}{dz} = -\rho g. \tag{4.9}$$

This, using Eq. 4.4 and taking $p = p_0$ at $z = H$ gives,

$$\rho = \rho_0[1 + \frac{6g\rho_0}{p_0 7}(H - z)]^{\frac{1}{6}}, \tag{4.10}$$

$$\approx \rho_0[1 + \frac{g\rho_0}{7p_0}(H - z)]. \tag{4.11}$$

Here we have used the binomial expansion to linearise the density profile. We can do this since, if our model is to be consistent, fractional variations in density must be small. We may still need to relax the initial solution (see Eq. 2.70) using some damping to obtain the desired "quiet start". In many cases, however, this is may not be necessary.

4.4 Modelling Solid Boundaries

It is quite straight forward to model solid boundaries, either stationary or in motion, with special boundary particles. When using SPH to model free surfaces, it is the relative motion of particles in the fluid which, through Eq. 2.25, changes the particle densities. Particles representing a solid boundary, then, should not contribute to the density of a particle. We simply need the boundary particles so prevent particles passing through the boundary without inhibiting their motion parallel to the boundary (assuming a free-slip boundary).

The first boundary particles employed (see [12]) exerted a radial force per unit mass of the form,

$$f(r) = \begin{cases} D\{(\frac{r_0}{r})^4 - (\frac{r_0}{r})^2\}\frac{\mathbf{r}}{r^2}, & \text{if } r \leq r_0; \\ 0, & \text{otherwise.} \end{cases} \tag{4.12}$$

Here, r_0 was chosen to be the initial particle spacing and D (with dimension velocity squared) was chosen to be comparable to or exceed the kinetic energy

per unit mass of the particles. So, for example, in the case of a breaking dam of height H, $D \approx 5gH$ was used.

This form of boundary force proved quite useful, but has some disadvantages. Since the boundary force is purely radial, particles can feel forces which have a component tangential to the boundary. Another way to look at this is that, a particle travelling parallel to the boundary will "perceive" it to be bumpy. This effect can result in artificial boundary layers close to the solid surface. This problem can be reduced (see [14]) by spacing the boundary particles at a third of the typical spacing of the SPH particles. This can become very expensive in higher dimensions and does not deal with a second problem concerning these boundary particles. As an SPH particle approaches such a boundary particle, the force exerted can become very large indeed, forcing a small time step to be used by the numerical integrator.

These problems are addressed by a new form of boundary particle first introduced in [16]. To make the boundary forces smooth, each boundary particle has an outward pointing unit normal $\mathbf{n}$ and exerts a force,

$$\mathbf{f} = f_1(\mathbf{n} \cdot \Delta\mathbf{r})P(\mathbf{t} \cdot \Delta\mathbf{r})\mathbf{n}. \tag{4.13}$$

The tangent vector $\mathbf{t}$ is readily constructed using $\mathbf{n}$ and $\Delta\mathbf{r}$. So, f_1 is responsible for repelling particles away from the boundary, while P is an interpolation function which "reinforces" the boundary force in between boundary particles.

The form suggested for f_1 is,

$$f_1(y) = \begin{cases} A(\frac{2\Delta x}{3y})^4, & \text{if } 0 < y \leq \frac{2\Delta x}{3}; \\ 9A(\frac{y}{\Delta x} - 1)^2, & \text{if } \frac{2\Delta x}{3} < y \leq \Delta x; \\ 0, & \text{otherwise,} \end{cases} \tag{4.14}$$

where Δx is the typical spacing between the SPH fluid particles. This boundary force and its first derivative are continuous. The magnitude of A will be dealt with shortly.

Many forms of interpolation function could be used, however, the Hamming window has been successful,

$$P(x) = \begin{cases} \frac{1}{2}(1 + cos(\frac{\pi x}{\Delta x})), & \text{if } |x| \leq \Delta x; \\ 0, & \text{otherwise.} \end{cases} \tag{4.15}$$

The co-efficient A should be chosen such that the resulting boundary forces do not place extra constraints on the time-step used by the numerical integrator. Normally (see Chapter 5) the Courant condition is the main constraint on the time step used. Thus, an A is used for which integration using the time step appropriate from the Courant condition is sufficiently accurate. We can get an estimate of the time step suitable for the boundary force by considering the gradient of the boundary force. If we let K denote $\frac{df_1}{dy}(2\Delta x/3)$, then a typical

time scale for motion within the field is $2\pi/\sqrt{|K|}$. This suggests a time-step of about $1/3\sqrt{|K|}$. If we equate this time step with one satisfying the Courant condition (i.e. $0.5h/c_s$), we find,

$$A = \frac{4{c_s}^2}{81h}. \tag{4.16}$$

Here we have taken $h = 1.5\Delta x$. Thus, the time step appropriate for integration of the boundary forces is comparable with that required for the SPH particle interactions. This means that the presence of the boundary particles places no extra constraints on the time step employed. Of course, the boundary force is unbounded if an SPH particle comes too close to a boundary particle. In this case, other constraints on the time step (see Chapter 5) will automatically reduce the time step. This should not happen, however, if p_0 has been chosen such that the Mach number of the flow is small.

At the join between two straight boundaries it is necessary to place a particle with an intermediate normal. Gently curving boundaries may be constructed with such particles. For surfaces with strong curvature, the interpolation between boundary particles is complicated slightly, but is still quite straight forward (see [16]).

Chapter 5

Time Integration

5.1 An Overview

The time integration of the SPH equations can be done using the same basic approaches which are employed for other explicit hydrodynamic methods. The chosen method should provide high order accuracy with a minimum number of sweeps over the particles. If, for example, ρ must is evaluated using Eq. 2.24, an extra sweep over the particles is required to obtain ρ before other interpolation can be carried out. By using a standard leap-frog or the predictor-corrector approach (see Section 5.2), second-order accuracy in time is achieved without requiring an excessive number of sweeps over the particles. The time step for the simulation is chosen according to the CFL (Courant, Friedrichs and Lewy) condition (see Section 5.2) so the time-integration is stable. In some applications, the time step required by the CFL condition varies greatly between different regions of the flow. In such cases it is possible to use individual time steps for the particles. If the time steps are chosen to fit a hierarchy of powers of 2, then it is relatively straight forward to integrate the equations of motion.

A second order Runge-Kutta integrator has also been used with SPH. In this case (see [2]) it is possible to use adaptive time stepping. The time step is chosen to minimise an estimate of the error in the integration within certain tolerances. The method requires more sweeps over the particles per time step, however. In practice, it turns out that this time step may be larger than that estimated using the CFL condition, and thus, this approach may have definite computational advantages. As has been pointed out previously, one of the advantages of using Eq. 2.25 is that it allows the density to be updated alongside other field quantities. It may then be possible to integrate Eq. 2.25 for several time steps and then occasionally correct with Eq. 2.24, to ensure conservation of mass.

Note that the stability properties discussed in Chapter 6 are independent of the time integrator used. Chapter 6 deals with instabilities which are inherent in the SPH equations for certain equations of state and certain kernels.

5.2 The Predictor Corrector Scheme

In this, one of the more popular integration schemes applied to SPH, the following equations are used to obtain the field quantities at the next time step,

$$\tilde{v}^{1/2} = v^0 + \frac{\Delta t}{2} f^0, \tag{5.1}$$

$$\tilde{x}^{1/2} = x^0 + \frac{\Delta t}{2} v^0, \tag{5.2}$$

$$\rho^{1/2} = \rho(\tilde{x}^{1/2}), \tag{5.3}$$

$$f^{1/2} = f(\tilde{x}^{1/2}, \tilde{v}^{1/2}, \rho^{1/2}, \ldots), \tag{5.4}$$

$$v^{1/2} = v^0 + \frac{\Delta t}{2} f^{1/2}, \tag{5.5}$$

$$x^{1/2} = x^0 + \frac{\Delta t}{2} v^{1/2}, \tag{5.6}$$

$$x^1 = 2x^{1/2} - x^0, \tag{5.7}$$

$$v^1 = 2v^{1/2} - v^0. \tag{5.8}$$

Here, the superscripts refer to the time step index, and f is the force. In practice we take $f^0 \approx f^{-1/2}$, since this reduces the work required without changing the order of the scheme.

The time step should be chosen to accommodate the CFL condition, which, essentially, states that the maximum rate of propagation of information numerically must exceed the physical rate. In SPH, this translates to,

$$\frac{h}{\Delta t} \geq c_s. \tag{5.9}$$

However, if viscosity is present, it should also be taken into account,

$$\Delta t_{cv} = \min_a \frac{h}{c_a + 0.6(\alpha c_a + \beta \max_b \mu_{ab})}. \tag{5.10}$$

To ensure that the forces exerted on individual particles are integrated correctly, the time step should also be less than,

$$\Delta t_f = \min_a (\frac{h_a}{|\mathbf{f}_a|}). \tag{5.11}$$

Here $\mathbf{f}_a$ is a force per unit mass (acceleration). So, a suitable time step for the scheme is,

$$\Delta t = \frac{1}{4} \min(\Delta t_{cv}, \Delta t_f). \tag{5.12}$$

The exact choice of coefficients can be varied slightly. For example, simulations suggest,

$$\Delta t = \min(0.4\Delta t_{cv}, 0.25\Delta t_f), \tag{5.13}$$

is adequate. If other processes are at work, for example heat conduction, then the time step should chosen to accommodate them using similar arguments. The main point to keep in mind is that the natural SPH length scale is h. Other scales for the phenomenon under consideration should be constructed from the relevant physical constants (as in Eq. 5.10).

Chapter 6

Stability properties of SPH

When using a formulation of SPH which conserves momentum exactly, the motion of the particles is observed to be unstable to negative stress. It is also found that, under normal circumstances, a lattice of SPH particles is potentially unstable to transverse waves. This chapter appears in [20] and is a summary of a detailed report ([19]) investigating the nature of these and other instabilities in depth. Approaches which may be used to eliminate these instabilities are suggested. It is found that the stability properties of SPH in general improve as higher order spline interpolants, approximating a Gaussian, are used as kernels. The early applications of SPH, [8] and [5], were to problems involving a compressible gas which always had a positive gas pressure. The equations governing the motion of the particles, when written in a form which conserves momentum exactly, result in particles repelling each other with equal and opposite forces. As particles approach, the density increases, the pressure increases, and the particles tend to repel each other. When applied to different problems where the stress can become negative the momentum conserving form of SPH is observed to become unstable to short wavelength perturbations. For negative stress, the particles no longer repel, but attract. Each particle is, in effect, at the bottom of a potential well, and it becomes possible for the particles to pair up and "slide" into each others wells, causing "clumping" initially and subsequently disrupting the solution. The nature of this instability is quite different from instabilities observed in explicit finite difference techniques when too large a time step is used. This SPH instability is a consequence of the particles being free to move under negative stress and is present even if the time integration is exact. Additional stability conditions, such as the Courant Friedrichs Levy condition must also be respected. Recently people have commented upon this instability in connection with many problems (e.g. elastic flow in [23]), but much earlier [21] had detected and studied the problem in connection with magnetohydrodynamics (MHD). Very little analytical work has been done in the study of the stability properties of SPH and previous methods (see [10]) actually break down in the region where the stability we seek to understand first appears. The report ([19]) extends the

stability analysis of SPH in order to not only understand the nature of potential instabilities but to give insight into how methods giving most accurate results may be formulated.

6.1 Seeking the Source of the Instability

In order to understand the problem better we must seek the fundamental source of instability. We have seen that the reported instability occurs when a stress tensor is implemented in a form which conserves momentum exactly. We will be considering one dimensional flows initially, with symmetric kernels. Typically, we might use a Gaussian kernel (Eq. 2.56) or the cubic spline interpolant (Eq. 2.58). Choosing a symmetric kernel guarantees exact conservation of momentum, since inter-particle forces then form action-reaction pairs.

Let us consider the specific case of one-dimensional MHD flow, with a constant magnetic induction B_0 parallel to the direction of the flow, say along the x-axis. Since the magnetic induction is constant, the equations of MHD reduce to those for hydrodynamics. However, the corresponding SPH equations may be written,

$$\begin{aligned} \frac{dv_a}{dt} &= -\sum_b m_b \left(\frac{p_a - \frac{1}{2\mu_0}B_0^2}{\rho_a^2} + \frac{p_b - \frac{1}{2\mu_0}B_0^2}{\rho_b^2} \right) \frac{\partial W_{ab}}{\partial x_a}, \\ \rho_a &= \sum_b m_b W_{ab}, \quad p_a = c^2 \rho_a, \\ W_{ab} &= W(x_a - x_b, h). \end{aligned} \tag{6.1}$$

So, in this case, the SPH equations for magnetohydrodynamical equations are equivalent to those for pure hydrodynamical flow with the pressure adjusted by a constant. Similar analysis may be done for any problem involving a stress tensor of similar form. So, the stability properties of one-dimensional Smooth Particle Magnetohydrodynamics (SPMHD) will be exhibited by the equations,

$$\begin{aligned} \frac{dv_a}{dt} &= -\sum_b m_b \left(\frac{p_a}{\rho_a^2} + \frac{p_b}{\rho_b^2} \right) \frac{\partial W_{ab}}{\partial x_a}, \\ \rho_a &= \sum_b m_b W_{ab}, \quad p_a = c^2 \rho_a + P, \end{aligned} \tag{6.2}$$

where $P = -B_0^2/2\mu_0$. Similar equations, with a different expression for P will be obtained by considering the one-dimensional case of other applications of SPH.

6.2 Stability Analysis and SPH

A simple way to analyse the stability of an implementation of SPH is to consider the dispersion relation for linear, sound waves propagating in a one-dimensional

flow. We can imagine an infinite line of identical particles oscillating about a constant mean separation. Such a wave may be described by,

$$x_a = a\Delta x + X\exp\left(ika\Delta x - i\omega t\right), \tag{6.3}$$

We now linearise Eqs. 6.2 by substituting Eq. 6.3 and neglecting all but first order terms to obtain,

$$\begin{aligned}\omega^2 = & \\ & \frac{2mc^2\Re}{\rho_0}\sum_j\left(1-\cos k\Delta xj\right)\frac{\partial^2 W}{\partial x^2}\left(\Delta xj,h\right) \\ & +\left(\frac{mc}{\rho_0}\right)^2\left(1-2\Re\right)\left\{\sum_j \sin k\Delta xj\frac{\partial W}{\partial x}\left(\Delta xj,h\right)\right\}^2,\end{aligned} \tag{6.4}$$

where we have chosen, $P = c^2\rho_0\left(\Re - 1\right)$. I have assumed W to be even (a more general expression is given in [19]). This choice of P gives,

$$p_a = c^2\rho_0\left(\frac{\rho_a}{\rho_0} - 1 + \Re\right). \tag{6.5}$$

We can think of the quantity $c^2\rho_0\Re$ as being the "background" pressure upon which the linear wave perturbations occur. Thus, if $\Re > 0$, then p_a should be positive for small perturbations and if $\Re < 0$, then p_a may become negative. $\Re$ will take different values depending on the equation of state being considered. For standard SPH, $\Re = 1$. For SPMHD, $\Re = 1 - B_0^2/2\mu_0 c^2\rho_0$. For incompressible SPH (see Chapter 4), $\Re = 0$. Using Poisson's summation formula, Eq. 6.4 may be written,

$$\begin{aligned}\omega^2 = & \\ & \frac{2mc^2\Re}{\rho_0\Delta x}\sum_{l=-\infty}^{+\infty}\left\{\left(k+\frac{2\pi l}{\Delta x}\right)^2 U\left(k+\frac{2\pi l}{\Delta x},h\right)\right. \\ & \qquad\left. -\left(\frac{2\pi l}{\Delta x}\right)^2 U\left(\frac{2\pi l}{\Delta x},h\right)\right\} \\ & +\left(\frac{mc}{\rho_0\Delta x}\right)^2\left(1-2\Re\right)\left\{\sum_{l=-\infty}^{+\infty}\left(k+\frac{2\pi l}{\Delta x}\right)U\left(k+\frac{2\pi l}{\Delta x},h\right)\right\}^2\end{aligned} \tag{6.6}$$

6.3 Stability of Another Formulation

It is possible to develop an alternative formulation to Eq. 6.2 which has stability properties independent of the background pressure,

$$\frac{dv_a}{dt} = -\sum_b m_b\frac{p_b - p_a}{\rho_a\rho_b}\frac{\partial W_{ab}}{\partial x_a}. \tag{6.7}$$

Since the differences of the pressures are taken in the momentum equation, Eq. 6.7, the value of $\Re$ is irrelevant. However, the forces exerted upon the particles according to Eq. 6.7 no longer form action-reaction pairs but are estimates of the local pressure gradient. Thus, this formulation does not conserve momentum exactly, except in the continuum limit (ie: $h \to 0$ and infinitely many particles). This pressure difference formulation has a very simple equation governing its stability,

$$\omega^2 = \left(\frac{mc}{\rho_0}\right)^2 \left[\sum_{j=-\infty}^{+\infty} \sin k\Delta x j \frac{\partial W}{\partial x}(\Delta x j, h)\right]^2 . \tag{6.8}$$

6.4 The Numerical Sound Speed

Ideally, we have $\omega^2 = c^2k^2$, thus it is useful to define,

$$C_{num}^2 = \frac{c_{num}^2}{c^2} = \frac{\omega^2}{k^2c^2}, \tag{6.9}$$

where c is the analytic sound speed. Ideally, of course, C_{num} should be as close to one as possible, so that sound waves are propagated realistically. If C_{num}^2 becomes negative, the perturbations in the numerical solution are no longer travelling waves, but are exponentially growing and decaying disturbances.

6.5 Results

It is clear that the dispersion relation is periodic in k with period $2\pi/\Delta x$. This is the result of aliasing, whereby waves of wavenumber k and $k + 2\pi/\Delta x$ look identical at a series of points separated by Δx. It has been established experimentally that the "problem" wavenumber is $\pi/\Delta x$ (a wavelength of two particle spacings). For $k = \pi/\Delta x$, Eq. 6.6, becomes,

$$\begin{aligned}\omega^2 &= \frac{2mc^2\Re}{\rho_0\Delta x}\sum_{l=-\infty}^{+\infty}\left\{\left(\frac{\pi(2l+1)}{\Delta x}\right)^2 U\left(\frac{\pi(2l+1)}{\Delta x}, h\right)\right. \\ &\qquad \left. - \left(\frac{2\pi l}{\Delta x}\right)^2 U\left(\frac{2\pi l}{\Delta x}, h\right)\right\}, \\ &= \frac{4mc^2\Re}{\rho_0}\sum_{j=-\infty}^{\infty}\frac{\partial^2 W}{\partial x^2}(\Delta x[2j+1], h). \end{aligned} \tag{6.10}$$

Eq. 6.10 shows that, for wavenumber $\pi/\Delta x$, the sign of ω^2, and hence C_{num}^2, changes sign with $\Re$. Thus, for any symmetric kernel, as the background pressure $c^2\rho_0\Re$ changes sign, it will change stability. There can be no kernel which is stable for both signs of $\Re$, using this implementation of SPH. Thus, to achieve general

stability for different background pressures, we must modify the kernel as $\Re$ changes sign. Let us consider Eq. 6.10 for the simple case where $W(\Delta xj, h) = 0$ for $|j| > 2$. Then,

$$\omega^2 = \frac{8mc^2\Re}{\rho_0}\frac{\partial^2 W}{\partial x^2}(\Delta x, h). \tag{6.11}$$

So, for this case, the sign of $\partial^2 W/\partial x^2(\Delta x, h)$ must change when the background pressure changes sign. This is particularly important to remember if we are seeking a kernel which changes continuously with $\Re$ to provide stability. The appropriate kernels for $\Re$ being slightly positive and slightly negative have different signs for $\partial^2 W/\partial x^2$, so $\partial^2 W/\partial x^2$ must be zero at the nearest neighbour when $\Re = 0$ for continuity. In the case of the Gaussian, we find that $\omega^2 = 0$ when $h = 2^{\frac{1}{2}}\Delta x$. Thus, varying the smoothing length may be sufficient to ensure stability for this wavenumber. A useful solution, however, must be stable for all wavenumbers.

We can see from the form of Eq. 6.4 that for any given h and k, C^2_{num} varies linearly with $\Re$. In general we wish C^2_{num} to vary only slowly with $\Re$, since, for the exact system, it is independent of $\Re$. It is informative to consider the quantity $\partial C^2_{num}/\partial\Re$, since this reflects the degree of dependence of the stability properties on $\Re$. For sufficiently large $\Re$ we have that $C^2_{num} \propto \Re$ where the constant of proportionality (for a given k and h) is $\partial C^2_{num}/\partial\Re$.

The limit of Eq. 6.6 as k approaches zero is of particular significance. It is in this limit that we expect our numerical method will resolve the wave best, since it corresponds to an infinite number of particles fitting into each wavelength. It can be shown that, in this limit, C^2_{num} is perturbed from 1 by a term which is linear in $\Re$ and proportional to the Fourier transform of the kernel evaluated at $2\pi/\Delta x$. The Fourier transform of the Gaussian kernel is, of course a Gaussian in kh, and, accordingly, falls off quite rapidly with kh. The Fourier transforms of kernels with compact support, however, do not fall off so rapidly, and we expect the sound speed to depend more strongly upon $\Re$ for such kernels. Numerical results obtained using direct summation in [19] of Eq. 6.4 confirm that C_{num} depends more strongly on $\Re$ for spline interpolated kernels. In fact, there are choices of k, Δx and h for which $\partial C^2_{num}/\partial\Re$ is negative. Thus, a sufficiently large choice of $\Re$ for such parameters results in C^2_{num} becoming negative, producing an instability. This result was not anticipated since it had been thought that SPH would be stable to any positive stresses. This instability resulting from over-pressure is of long wavelength and, correspondingly, can have a serious affect upon the accuracy of large scale phenomena. The use of smoother spline approximations to a Gaussian kernel increases the over-pressure required to induce the instability. More details on these results may be found in [19].

6.6 Mutating the Kernel

We have seen that no single kernel can provide us with the stability we seek. We need some way of modifying the present Gaussian shaped kernel. Any kernel, $W(x,h)$ we choose must have the following properties (in one-dimension):

$$\int_{-\infty}^{+\infty} W(x,h)dx = 1, \quad \lim_{h\to 0} W(x,h) = \delta(x), \tag{6.12}$$

and, if we wish momentum to be conserved exactly,

$$W(x,h) = W(-x,h). \tag{6.13}$$

Suppose that our "favourite" kernel is,

$$W_0(x,h) = \frac{1}{h} f\left(\frac{x}{h}\right), \tag{6.14}$$

We can now define an infinite series of symmetric kernels satisfying Eqs. 6.12 of the following form,

$$W_n(x,h) = \frac{A_n}{h}\left(\frac{x}{h}\right)^{2n} f\left(\frac{x}{h}\right), \tag{6.15}$$

where A_n is chosen to satisfy Eq. 6.12. Now we have a set of kernels which we can combine to form a kernel with the necessary properties for stability,

$$W(x,h) = \sum_{j=0}^{N} B_n W_n(x,h), \tag{6.16}$$

where,

$$\sum_{j=0}^{N} B_n = 1. \tag{6.17}$$

We need to develop some method for choosing the co-efficients B_n such that the resulting kernel has the desired stability properties. One possible approach is to choose several points that we want $\omega(k)$ to pass through. We then solve for the same number of free co-efficients as we have conditions by linearising about an initial guess and solving the resultant linear system of equations. We continue this iterative process until sufficient convergence is achieved. There are some conditions which must be respected in order that the system converges. These, and other details, are explored in [19].

6.7 The Pressure Differencing Formulation of SPH

The form of Eq. 6.8 ensures that the formulation Eq. 6.7 is always stable. It can also be shown that the sound speed for this implementation depends less

strongly upon the particle spacing and smoothing length than the exactly momentum conserving formulation. This implementation, of course, has stability independent of $\Re$ since all pressures appear as differences in Eq. 6.7. However, it does not conserve momentum exactly and, thus, is not as good as the momentum conserving formulation (see [22]) for modelling strong shocks. The pressure differencing formulation exhibits much larger oscillations when modelling strong shocks, though these might be tamed by using a different form of viscosity. The exactly momentum conserving method calculates the net particle forces as the sum of individual repelling interactions. This is less subject to oscillations than a method where the forces exerted on the particles are calculated from an estimate of the pressure gradient. When modelling stronger shocks, the pressure differencing formulation becomes less accurate as exact conservation of momentum becomes more necessary.

6.8 Stability Analysis with Variable Particle Spacing

In practice, a simulation will not involve particles oscillating about a constant separation. In order to deal with a number of different particle spacings we could solve for a kernel appropriate to each particle spacing and then use symmetric combinations of these when particles interact. If the expression Eq. 6.4 is used to find appropriate kernels, it is found that the numerical sound speed is significantly reduced. Effectively, the kernel is being changed continuously in such a fashion as to slightly oppose the propagation of the wave. If, however, we reformulate the stability analysis to include the assumption that the kernel is a function of the particle spacing, the sound speed will be more accurate. We need an appropriate variable to reflect the local spacing of particles. The distance to a nearest neighbour and other similar quantities are quite clumsy to use for such analysis. The specific volume,

$$V_a = \frac{m}{\rho_a}, \tag{6.18}$$

is much more suitable. We now consider Eqs. 6.2 with the consideration that,

$$W_{ab} = W\left(x_{ab}, h, V_{ab}\right), V_{ab} = \frac{1}{2}\left(V_a + V_b\right). \tag{6.19}$$

Applying stability analysis to the resulting SPH equations, allows us to obtain a somewhat complicated dispersion relation. An appropriate form for the kernel can be derived in a similar fashion to that employed in the case of constant particle separation.

6.9 Stability Analysis with Viscosity

One might think that introducing viscosity to the equations of motion might eliminate the instability resulting from negative stress. In particular, since the first instability is of short wavelength ($k \approx \pi/\Delta x$) we would expect viscosity to have a strong damping effect upon it. Let us consider the previous equations with the addition of artificial viscosity,

$$\begin{aligned} \frac{dv_a}{dt} &= -\sum_b m_b \left(\frac{p_a}{\rho_a^2} + \frac{p_b}{\rho_b^2} + \Pi_{ab} \right) \frac{\partial W_{ab}}{\partial x_a}, \\ \Pi_{ab} &= -\frac{\alpha c \mu_{ab}}{\frac{1}{2}(\rho_a + \rho_b)}, \mu_{ab} = \frac{h v_{ab} x_{ab}}{x_{ab}^2 + \eta^2}. \end{aligned} \tag{6.20}$$

Once again, we consider a linear wave perturbing an infinite line of particles parallel to the x-axis and obtain the following dispersion relation,

$$\omega^2 + ia\omega - b = 0, \tag{6.21}$$

where,

$$a = -\frac{m\alpha ch}{\rho_0 \Delta x} \sum_{j \setminus \{0\}} \frac{1 - \cos k\Delta x j}{j} \frac{\partial W}{\partial x}, \tag{6.22}$$

and

$$\begin{aligned} b &= \frac{2mc^2 \Re}{\rho_0} \sum_j (1 - \cos k\Delta x j) \frac{\partial^2 W}{\partial x^2} \\ &\quad + \left(\frac{mc}{\rho_0} \right)^2 (1 - 2\Re) \left[\sum_j \sin k\Delta x j \frac{\partial W}{\partial x} \right]^2. \end{aligned} \tag{6.23}$$

The definitions of a and b are chosen such that they are real and, for the standard kernel and $\Re = 1$, are positive. Thus, we have,

$$\omega = \pm \frac{(4b - a^2)^{\frac{1}{2}}}{2} - i\frac{a}{2}. \tag{6.24}$$

From Eq. 6.3 we find,

$$v = V \exp(ikx - i\omega t) = V \exp\left(ikx \mp i \frac{(4b - a^2)^{\frac{1}{2}}}{2} t - \frac{a}{2} t \right). \tag{6.25}$$

We see that a is responsible for dampening the motion and reducing the speed of propagation. Let us now consider the crucial wavenumber, $k = \pi/\Delta x$. Substituting into Eqs. 6.22 and 6.23 we obtain,

$$\begin{aligned} a &= -\frac{m\alpha ch}{\rho_0 \Delta x} \sum_{j \setminus \{0\}} \frac{1 - (-1)^j}{j} \frac{\partial W}{\partial x}, \\ b &= \frac{2mc^2 \Re}{\rho_0} \sum_j (1 - (-1)^j) \frac{\partial^2 W}{\partial x^2}. \end{aligned} \tag{6.26}$$

Typically if $\Re < 0$ (ie: negative stress) then $b < 0$. Thus, we obtain,

$$\omega = \pm i\frac{(4\beta + a^2)^{\frac{1}{2}}}{2} - i\frac{a}{2}, \tag{6.27}$$

where $\beta = -b$. The component of this which leads to the instability is,

$$\omega = \frac{i}{2}\left(\left(4\beta + a^2\right)^{\frac{1}{2}} - a\right), \tag{6.28}$$

So we see that the instability is not removed by the introduction of viscosity. If $a^2/4\beta \ll 1$ then

$$\omega \approx i\left(\beta^{\frac{1}{2}} - \left(\frac{a}{2} - \frac{a^2}{8\beta}\right)\right). \tag{6.29}$$

If $a/2 > a^2/8\beta$, then we see that the effect of introducing a small amount of viscosity is to reduce the growth rate of the instability.

6.10 Two Dimensional Stability Analysis

Let's consider the stability properties of standard two dimensional isothermal SPH,

$$\begin{aligned}
\frac{d\mathbf{v}_{ab}}{dt} &= -\sum_c \sum_d m_{cd}\left(\frac{p_{ab}}{\rho_{ab}^2} + \frac{p_{cd}}{\rho_{cd}^2}\right)\nabla_{ab} W_{abcd} \\
p_{ab} &= c^2 \rho_{ab}, \quad \rho_{ab} = \sum_c \sum_d m_{cd} W_{abcd} \\
W_{abcd} &= W\left(x_{ab} - x_{cd}, y_{ab} - y_{cd}, h\right)
\end{aligned} \tag{6.30}$$

We can analyse the stability of a rectangular lattice of particles by considering the propagation of plane waves on such a grid,

$$\begin{aligned}
x_{ab} &= a\Delta x + X\exp\left(ik_x a\Delta x + ik_y b\Delta y - i\omega t\right), \\
y_{ab} &= b\Delta y + Y\exp\left(ik_x a\Delta x + ik_y b\Delta y - i\omega t\right).
\end{aligned} \tag{6.31}$$

Proceeding in a similar fashion to the one dimensional analysis we obtain two solutions for each pair of k_x and k_y. The full details are in [19], but let us consider the dispersion relation obtained for plane waves propagating along the x-axis. We find that there is a longitudinal wave solution,

$$\begin{aligned}
\omega^2 &= \frac{mc^2}{\rho_0} 2\sum_i \sum_j \left(1 - \cos k\Delta x i\right)\frac{\partial^2 W}{\partial x^2} \\
&\quad - \left(\frac{mc}{\rho_0}\right)^2 \left\{\sum_i \sum_j \sin k\Delta x i \frac{\partial W}{\partial x}\right\}^2,
\end{aligned} \tag{6.32}$$

which corresponds to the one dimensional result Eq. 6.4 with $\Re = 1$ and the kernel replaced by a sum over j of the kernel. It turns out that this finite approximation to the y integration of the kernel introduces some small instabilities for large $h/\Delta x$. The system also supports a transverse wave with the dispersion relation,

$$\omega^2 = \frac{mc^2}{\rho_0} 2 \sum_i \sum_j (1 - \cos k\Delta xi) \frac{\partial^2 W}{\partial y^2}. \tag{6.33}$$

These waves, of course, are not present in the exact solution to the wave equation for an isothermal gas, but they are present in our lattice approximating an isothermal gas. Their presence is the result of variations in the value of the gradient of the kernel as particles "jostle" around. It turns out (see [19]) that for spline interpolated kernels ω^2 is negative for about half of the choices of h for a given Δx. The growth rate of these instabilities is radically reduced as higher order spline interpolants are used. If the Gaussian is employed the growth rate of these unstable transverse modes is negligible for all practical choices of smoothing length. This would suggest that, once again, the stability properties of SPH are improved by using kernels whose Fourier transform falls off more rapidly.

It is interesting to note that the standard implementation of viscosity has no effect on linear transverse waves. The stability properties of hexagonal lattices have also been considered in [19] with somewhat similar results. Three dimensional stability analysis also reveals unstable transverse modes which are reduced by the use of higher order spline interpolants. It can also be shown that the pressure differencing formulation does not exhibit these instabilities.

6.11 Conclusion

It is observed that the stability properties of SPH are improved by the use of kernels whose Fourier transforms fall off more rapidly. The instability first observed in exactly momentum conserving SPMHD in [21] can be reproduced by a simple artificial equation of state (Eq. 6.2). There are many applications which involve an equation of state having the effect of adjusting the background pressure acting between particles. Some examples are MHD, incompressible SPH, elastic-plastic flow and problems where we model a fluid experiencing an external pressure. The pressure adjustment, when SPH is implemented in an exactly momentum conserving form, influences the propagation of waves within the medium but this influence is reduced by the use of higher order spline interpolated kernels. Once the stress acting between particles changes sign, however, a different kernel must be used. It is possible to construct a kernel which varies with the stress acting between particles so as to ensure stability and realistic wave propagation. However, for complicated equations of state in two or three dimensions, this may not be feasible. Formulations of SPH which calculate the stress gradients by taking differences between the stress at neighbouring particles are observed to simulate

the propagation of waves very well. The simulation of strong shocks, however, suffers since momentum is no longer conserved exactly. In many circumstances it may be best to split the stress tensor into a component which is always positive and evaluate the remainder using a differencing formulation. For example, in the case of MHD the magnetic pressure could be added to the hydrodynamic pressure and employed in an exactly momentum conserving form. This would permit the simulation of strong shocks for which pressure forces are dominant. It may also be possible to adjust the stress at each of the particles by a constant, so as to ensure it is positive everywhere, thus permitting exact momentum conservation. However, if the adjustment is extreme, a higher order spline interpolated kernel my be required in order to avoid instabilities and strong dispersive effects. Boundary conditions may also become complicated.

For all two dimensional and three dimensional applications using an exactly momentum conserving form, the use of kernels with compact support introduces instabilities in transverse modes on rectangular and hexagonal lattices of particles. The growth rates of these instabilities are observed to decrease dramatically as higher order spline approximations to the Gaussian are employed. These instabilities are not exhibited by differencing formulations.

In general, kernels more closely approximating a Gaussian will give better results, but will cost more computationally as the number of contributing neighbours increases. However, this cost may be offset since such kernels may permit a decrease in h. It is important to have an understanding of the detail one wishes to resolve in a given problem. This understanding combined with sound knowledge of the stability and accuracy of the method employed allows us to have confidence in the results obtained.

Bibliography

[1] G. K. Batchelor. *An Introduction to Fluid Dynamics.* (Cambridge Univ. Press, Cambridge, UK, 1973).

[2] W. Benz. *Astron. Astrophys.*, 139:378, 1984.

[3] W. Benz. Smooth particle hydrodynamics: A review. page 269, 1989. Nato Workshop, Les Arcs, France.

[4] G. V. Bicknell. *SIAM J. Sci. Stat. Comput.*, 12:1198, 1991.

[5] R. A. Gingold and J. J. Monaghan. *MNRAS*, 181:375, 1977.

[6] R. A. Gingold and J. J. Monaghan. *J. Comput. Phys.*, 46:429, 1982.

[7] L. Hernquist and N. Katz. *Ap. J. Suppl.*, 70:419, 1989.

[8] L. B. Lucy. *AJ*, 83:1013, 1977.

[9] J. J. Monaghan. *Comput. Phys. Rep.*, 3(2):71, 1985.

[10] J. J. Monaghan. *J. Comp. Phys.*, 82:1, 1989.

[11] J. J. Monaghan. Smoothed particle hydrodynamics. *Annu. Rev. Astron. Astrophys.*, 30:543–74, 1992.

[12] J. J. Monaghan. *J. Comp. Phys.*, 110:399, 1994.

[13] J. J. Monaghan. Heat conduction with discontinuous conductivity. *Applied Mathematics Reports and Preprints, Monash University*, (95/18), 1995.

[14] J. J. Monaghan. Simulating gravity currents with SPH: III boundary forces. *Applied Mathematics Reports and Preprints, Monash University*, (95/7), 1995.

[15] J. J. Monaghan. Simulating gravity currents with SPH lock gates. *Applied Mathematics Reports and Preprints, Monash University*, (95/5), 1995.

[16] J. J. Monaghan. Improved modelling of boundaries. *SPH Technical Note, CSIRO Division of Mathematics and Statistics*, May 31, 1995.

[17] J. J. Monaghan and J. C. Lattanzio. *Astron. Astrophys.*, 149:135, 1985.

[18] J. J. Monaghan and J. P. Morris. Shock detection with SPH. to be published.

[19] J. P. Morris. A study of the stability properties of SPH. *Applied Mathematics Reports and Preprints, Monash University*, (94/22), 1994.

[20] J. P. Morris. *Pub. Ast. Soc. Australia*, 1995. accepted for publication.

[21] G. W. Phillips and J. J. Monaghan. *MNRAS*, 216:883, 1985.

[22] M. Steinmetz and E. Mueller. *A&A*, 268:391, 1993.

[23] J. W. Swegle. *Report at Sandia National Laboratories*, 1992. August 13, to be published.